HHS Public Access

Author manuscript

Int J Prosthodont. Author manuscript; available in PMC 2023 July 01.

Published in final edited form as:

Int J Prosthodont. 2022 ; 35(4): 469–479. doi:10.11607/ijp.7551.

Effect of Porcelain-to-Zirconia Ratio and Bonding Strategy on the Biaxial Flexural Strength and Weibull Characteristics of a Stress-Free Bilayer CAD/CAM Ceramic System

Tabata Prado Sato, DDS, MSc, PhD(c),
Institute of Science and Technology, Universidade Estadual Paulista, São José dos Campos, Brazil.

Anelyse Arata, DDS, MSc, PhD(c),
Nanoscience and Advanced Materials Program, Federal University of ABC, Bangú, Brazil.

Larissa Mendonça de Miranda, MSc, PhD,
Federal University of Rio Grande do Norte, Department of Dentistry, Division of Prosthodontics, Natal, Brazil.

Marco Antonio Bottino, DDS,
Department of Dental Materials Institute of Science and Technology, University Estadual Paulista, São José dos Campos, Brazil.

Renata Marques de Melo, DDS,
Department of Dental Materials Institute of Science and Technology, University Estadual Paulista, São José dos Campos, Brazil.

Yu Zhang [Prof],
University of Pennsylvania, School of Dental Medicine, Department of Preventive and Restorative Sciences, Philadelphia, Pennsylvania, USA.

Rodrigo Othávio Assunção Souza, MSc, PhD
Department of Dentistry, Federal University of Rio Grande do Norte, Rio Grande do Norte, Brazil.

Abstract

Purpose: To evaluate the biaxial flexural strength of different porcelain-to-zirconia thickness ratios and bonding strategies of a stress-free bilayer CAD/CAM ceramic system.

Materials and Methods: A total of 60 zirconia discs (diameter: 15 mm; thickness: 0.3 or 0.5 mm; n = 30 for each thickness) were divided into six groups (n = 10 each) according to porcelain-to-zirconia ratio and bonding strategy: VM/Zr (control): zirconia discs veneered with a feldspathic ceramic (VM 9, Vita) in 0.9-mm and 0.7-mm thicknesses using a conventional hand-layering technique; VB/Zr-SBU: zirconia discs airborne particle–abraded with 50-μm Al_2O_3 particles followed by an MDP primer application (Single Bond Universal, 3M) and bonded to the porcelain with a resin cement (Panavia F 2.0, Kuraray); and VB/Zr-RC: zirconia discs airborne particle–abraded with 30-μm silica-coated Al_2O_3 particles and silanized and bonded to the porcelain with

Correspondence to: Adjunct Prof Rodrigo O. A. Souza Federal University of Rio Grande do Norte (UFRN), Department of Dentistry Av. Salgado Filho, 1787, Lagoa Nova, Natal / RN 59056-000, Brazil, rodrigoothavio@gmaii.com.

the same resin cement. Before cementation, the VB (Vitablocs II) discs were etched with 5% hydrofluoric acid (60 seconds), followed by silane application. The bilayers (thickness = 1.2 mm) were loaded with 750 g while light curing the resin cement. Two porcelain-to-zirconia thickness ratios were evaluated: 0.9: 0.3 mm and 0.7: 0.5 mm. All groups were subjected to 106 mechanical cycles, followed by a biaxial flexural test. Data (MPa) were subjected to two-way analysis of variance (ANOVA), Tukey test (5%), and Weibull analyses.

Results: Two-way ANOVA revealed that the factor porcelain-to-zirconia ratio ($P = .0556$) was not significant; however, the bonding strategy factor was statistically significant. Among the 0.5-mm zirconia groups, the VB/Zr-SBU group presented higher flexural strength (s) than the VM/Zr or VB/Zr-RC groups. Similar results were also found for the 0.3-mm zirconia groups, in which the VB/Zr-SBU group also presented higher strength than the others, which were similar in comparison (Tukey). The Weibull modulus was similar among the groups; however, the characteristic strength was significantly different ($P = .000$).

Conclusion: The zirconia bonding strategy with 50-μm Al_2O_3 airborne-particle abrasion, followed by a primer application, increases the flexural strength of a stress-free bilayer CAD/CAM ceramic system.

Yttria-stabilized tetragonal zirconia polycrystal (3Y-TZP) is a highly crystalline material with outstanding mechanical properties (ie, high flexural strength, fracture toughness, and hardness)[1] compared to other ceramics used in dentistry.[2,3] These characteristics mainly result from the phase transformation toughening mechanisms.[1,4]

However, several clinical studies have reported a higher chipping prevalence with veneering ceramics, which vary according to clinical trials: for crowns, chipping accounts for 71% of the failures found in 2 years[5] and 11.7% of the failures found in 12 years[6]; for fixed partial dentures, chipping of the ceramic coating accounts for 13% of the failures in 3 years[7] and 15.2% of the failures in 5 years[8] for restorations in posterior areas. According to the literature, chipping is the most common failure in zirconia restorations.[9,10] The etiology of chipping is still unclear; however, several factors are related to this type of failure, such as residual thermal stress because of the differences in the coefficient of thermal expansion (CTE)[11] and the elastic modulus between the veneering ceramic and zirconia,[12,13] the cooling rate,[13] the geometry of the bilayered restoration,[14] the thickness and type of veneering ceramic,[13,15] the processing technique of the veneering ceramic,[16] the framework support, and sliding contact fatigue.[11,17]

Considering that traditional Y-TZP has low translucence,[18,19] the veneering ceramic must be applied over the framework. This is usually done through the hand-layered stratified technique, in which layers of powder and liquid mixture are applied and sintered. An alternative is the pressed technique, in which a veneering ceramic is injected over the framework that is included in the investing material. The stratified technique demands technical skills, is more prone to the inclusion of porosities than the pressed technique, and generally requires multiple firings. However, the pressed technique does not increase the ceramic's flexural strength.[15]

Thus, several methods have been suggested to eliminate or decrease the residual stress in an effort to reduce the risk of chipping the veneering ceramic, such as the CAD-on technique and CAD/CAM rapid layer manufacturing (RLM). In the CAD-on technique, a special glass-ceramic is fused at the zirconia–lithium disilicate ceramic[9] interface where both the veneer and core structures were previously milled by a CAD/CAM system, reducing the residual stress. Alessandretti et al[20] reported that the CAD-on technique presented a low chipping rate compared to the conventional bilayer technique. On the other hand, with RLM,[16] the zirconia coping and the feldspathic veneered ceramic—also previously milled separately—are adhesively bonded with resin cement, thereby eliminating residual stresses altogether. This technique also allows for resin penetration into the veneering ceramic,[21] leading to crack growth inhibition at the resin interlayer interface.[16] According to the manufacturer, RLM reduces or eliminates chipping and failures due to the materials' different CTEs. Kobayashi et al[22] demonstrated that an indirect composite material's bond strength to zirconia ceramics could be above the threshold for clinically acceptable composite-metal or ceramic bonds.

Considering that the literature regarding RLM is scarce and that this technique requires a very effective and durable adhesive between the zirconia and the ceramic veneer, bonding strategies for these materials must be evaluated to predict the clinical long-term stability/outcome of this type of restoration. Moreover, to the best of the present authors' knowledge, different porcelain-to-zirconia thickness ratios using the RLM technique have not yet been evaluated. Therefore, the hypotheses of this study were: *(1)* the porcelain-to-zirconia thickness ratios in the stress-free bilayer CAD/CAM ceramic groups affect their flexural strength; and *(2)* the bonding strategies of the stress-free bilayer CAD/CAM ceramic groups result in higher flexural strength than the conventional hand-layered technique.

MATERIALS AND METHODS

All of the materials used in the study are shown in Table 1. The flowchart of the experimental design of this study is shown in Fig 1.

Specimen Preparation

Presintered zirconia ceramic blocks (Zr; 14 × 15 × 20 mm) for CAD/CAM were machined into cylinders (15-mm diameter) using wet-finished silicon carbide sandpapers (120-, 400-, and 600-grit) in a polishing machine (Buehler). The 3Y-TZP cylinders were cut into discs of two different thicknesses (0.3 mm or 0.5 mm; n = 30 each; Fig 2) using a precision cutting machine (IsoMet 1000, Buehler). Next, the parallel surfaces of the ceramic discs were ground with silicon carbide (SiC) wet sandpapers (120-, 400-, 600-, 800-, and 1,200-grit), washed in water, and left to dry at 180°C for 30 minutes. The discs were subsequently sintered at 1,530°C for 2 hours in a high-temperature furnace (Vita Zyrcomat, Vita Zahnfabrik) according to the manufacturer's instructions. All specimens were immersed in distilled water and cleaned in an ultrasonic bath for 2 minutes (Vitasonic, Vita Zahnfabrik).

Feldspar ceramic blocks (Vitabloc Mark II, Vita Zahnfabrik; VB) were rounded into 12-mm–diameter cylinders using wet SiC papers (120-, 400-, 600-, 800-, and 1,200-grit) under water cooling. The cylinders were then cut into discs with two different thicknesses (0.9

mm or 0.7 mm; n = 20 each; Fig 2) using a precision cutting machine. Specimens were wet finished using SiC papers (120-, 400-, 600-, 800-, and 1200-grit). All discs were immersed in distilled water and cleaned in an ultrasonic bath for 2 minutes (Vitasonic, Vita Zahnfabrik).

Bonding Strategy

The bonding strategy varied according to experimental group:

- Control groups (VM/Zr): a hand-layered ceramic powder (VM 9, Vita Zahnfabrik) was mixed with modeling liquid and applied to the Zr disc surface to build up a bilayer with a final thickness of 1.2 mm. Next, 0.9 and 0.7 mm of VM 9 was applied onto the Zr discs with 0.3-mm and 0.5-mm thicknesses, respectively. The ceramic discs were sintered following the manufacturer's instructions for the first and second individualized firing cycles for VM 9 veneering ceramic at 930°C and 920°C, respectively (Table 2).
- VB/Zr-SBU: The VB discs (0.9-mm and 0.7-mm thickness) were etched with 5% hydrofluoric acid (HF) for 60 seconds, washed with water jets for 60 seconds, and air dried. Next, a thin layer of universal adhesive (ScotchBond Universal [SBU], 3M ESPE) was applied onto the etched surface with a microbrush and brushed for 20 seconds, followed by light air jets for 5 seconds for solvent evaporation and light curing for 10 seconds (1,400 mW/cm), according to the manufacturer's instructions (Fig 2). The zirconia specimen surfaces were then airborne particle–abraded with 50-μm aluminum oxide particles (Al_2O_3) for 30 seconds under 2.8-bar pressure, rinsed with tap water for 15 seconds and dried, and then a thin layer of universal adhesive (SBU) was also applied and light cured for 10 seconds. A thin layer of resin cement (Panavia F 2.0, Kuraray Noritake) was applied to both bonding surfaces, and the bilayers were loaded with 750 g to create a uniform layer of resin cement. Then, the excess resin cement was removed and light cured (Valo; 1,400 mW/cm^2) around the assemblies (0, 90, 180, and 270 degrees) for a total of 40 seconds. Light curing was then performed on the top surface for 20 seconds after the load removal. The Zr discs with 0.3-mm and 0.5-mm thicknesses were bonded to VB with 0.9- and 0.7-mm thicknesses, respectively (Fig 2), to ensure the bilayer specimen had a final thickness of 1.2 mm.
- VB/Zr-RC: The VB discs (0.9- and 0.7-mm thickness) were also etched with 5% hydrofluoric acid (HF) for 60 seconds, washed with water jets for 60 seconds, air dried, and silanized (Monobond Plus, Ivoclar Vivadent). The zirconia surfaces were then airborne particle–abraded with 30-μm silica-coated Al_2O_3 particles (Rocatec, 3M) for 15 seconds under 2.8-bar pressure, followed by silane application (Monobond Plus). A thin layer of resin cement (Panavia F 2.0, Kuraray Noritake) was applied and light cured as previously described. The Zr discs with 0.3- and 0.5-mm thicknesses were bonded to VB with 0.9- and 0.7-mm thicknesses, respectively, to ensure the bilayer specimen had a final thickness of 1.2 mm.

Mechanical Cycling

All specimens were subjected to cyclic loading in a mechanical fatigue simulator (ER-11000 Plus, ERIOS Equipamentos Técnicos e Científicos). The samples were placed, with the zirconia layer facing downward, on three supporting steel balls housed in a metallic base, which also presented three lateral rods to avoid specimen dislocation during fatigue testing. The supporting balls were 3.2 mm in diameter and spaced equidistantly from each other (ISO 6872).[23] Load was applied at the center of the top porcelain surface through a 1.6-mm diameter piston. An oscillating load (between 0 and 100 N) was applied for 10^6 cycles at a frequency of 2 Hz. The testing device was placed on the base of the fatigue machine with a thermostat, allowing fatigue testing to be carried out in an aqueous medium at a constant temperature of 37°C.

Biaxial Flexural Mechanical Test and Fracture Analysis

After the fatigue cycles were completed, the specimens were subjected to a biaxial flexural strength (BFS) test in a universal testing machine (EMIC, DL-1000) at a speed of 1 mm/minute and load cell of 1,000 kgf until fracture of the specimens. The set-up for biaxial flexural testing was made according to ISO 6872.[23] In all cases, the zirconia surface was placed downward (under tensile stress) during the flexural test. The top surface was covered with a tape to avoid cone cracking. The testing was interrupted at the first sound of cracking, which usually corresponded to the fracture at the bottom porcelain layer.

The stress-moment relation was calculated following Hsueh's solution for bilayers.[24] The stress distribution along the loading axis across the layers was then calculated using Matlab to plot the graph (MathWorks). Stresses at the top, bottom, and interfaces were calculated using Hsueh's solutions.[24] The lower surface (porcelain) strength data were subjected to descriptive and inferential statistical analyses.

Next, the stress-moment relation for the experimental groups was calculated according to Hsueh's solutions[25]:

$$\sigma_i = \frac{E_i(z - z^*)M}{(1 - \vartheta_i)(1 + \vartheta)\, D^*} (i = 1 to n)$$

In the formula, i is the layer number, z* is the position of the neutral plane, M is the bending moment per unit length, D* is the flexural rigidity, and υ is the Poisson ratio of the multilayer.

The stress distribution was then calculated based on the above equation using the elastic modulus and Poisson ratio for each material.[26,27]

The specimens were further evaluated in a stereomicroscope (Discovery z-20, Zeiss) and using scanning electron microscopy (SEM, Inspect S 50, FEI) operating at 20 to 25 kV, 5.0 spot, for observation of the interfaces. The failure analysis (SEM) of surface treatments was performed through qualitative descriptive analysis.

Statistical Analyses

The sample power was calculated through the website www.openepi.com, considering a 95% CI. The data obtained (MPa) from BFS were submitted to the analysis of variance (ANOVA) statistical model after considering the distribution of residuals (Levene test) using the Minitab software program (version 17, 2013). Two-way ANOVA and post hoc Tukey test (both $\alpha = 5\%$) analyzed the BFS for each zirconia ratio using the Statistix program (version 8.0, 2003, Analytical Software).

Weibull modulus (m) and characteristic strength (σ_0) were obtained by a Weibull analysis for flexural strength, which indicates the material's microstructural homogeneity considering strength variation. The characteristic strength is the strength at a failure probability of approximately 63.3%. Weibull modulus and characteristic strength with a 95% CI were calculated by the ln{ln [1/(1 − F(σc)]} vs. lnσc diagram (according to ENV 843-5):

$$lnln\left(\frac{1}{1 - F(\sigma_c)}\right) = mln\sigma_c - mln\sigma_0$$

The *P* values of Weibull modulus (m) and characteristic strength (σ_0) were calculated using chi-square test. The statistical analysis was performed in the Minitab software with a significance level set at 5%.

RESULTS

The sample power calculation was 100%. Levene test revealed no statistically significant difference among the SD values ($P > .05$). These results relate that the data followed a normal distribution ($P = .096$).

Two-way ANOVA revealed that the porcelain-to-zirconia ratio ($P = .0556$) and bonding strategy x porcelain-to-zirconia ratio interaction ($P = .3533$) were not significant. However, the bonding strategy factor was statistically significant ($P = .0000$) (Table 3). When only the factor bonding strategy was considered, the Al_2O_3 followed by SBU application (649.55 MPa)^A promoted statistically higher flexural strength than the silica-coated Al_2O_3 (493.29 MPa)^B and no treatment (421.30 MPa)^B groups, which were similar when compared to each other (Tukey test).

ANOVA (one-way) showed that when the 0.5-mm zirconia groups were compared, VB/Zr-SBU (636.55 ± 98.02$^\alpha$) presented higher strength than VM/Zr (489.25 ± 66.45$^\gamma$) and VB/Zr-RC (344.05 ± 98.02$^\beta$), which were also different ($P = .000$; Tukey). Similar results were also found in the 0.3-mm zirconia groups, where VB/Zr-SBU (698.4 ± 194.85$^\alpha$) also presented higher strength than the other groups (VM/Zr: 497.33 ± 143.15$^\beta$ and VB/Zr-RC: 471.48 ± 151.82$^\beta$), which were similar when compared to each other ($P = .0087$; Tukey) (Table 4).

Weibull distributions are graphically presented in Fig 3. The Weibull modulus was similar among the groups ($P > .05$); however, the characteristic strength ($P = .000$) was significantly

higher for the VB/Zr-SBU group (0.3-mm Zr = 767.5[a] MPa; 0.5-mm Zr = 675.3[a] MPa) than the VB/Zr-RC (373.5[c] MPa) and VB/Zr (515.8[b] MPa) groups with 0.5-mm Zr.

The failure analyses showed that porcelain cracking without delamination or debonding from the zirconia was the most common failure mode. When zirconia fractured during the test, the complete fracture of some discs was observed in the interface. Figure 4 shows the specimen interfaces under SEM.

DISCUSSION

Flexural strength is a method standardized by ISO 6872/15[23] to assess the mechanical strength of dental ceramics[28] using different tests: 3-[29] and 4-bending test,[30] and BFS.[31] BFS is considered a reliable test and has been used by several studies in the literature.[31,32] Its main advantages are applying force in a concentric point of the sample, multiaxial stress distribution,[33] eliminating possible flaws in the sample edges,[33,34] and resulting in a more uniform analysis of the material[35,36] to better predict the clinical performance of the ceramic material.[34] Thus, this test was selected in the present study.

One of the main factors contributing to material fracture is fatigue, which is defined as a subcritical crack where there is a growth of pre-existing defects in the ceramic material[36] triggered by intermittent loading below the resistance to fracture of the material in an aqueous environment.[37] This type of failure is simulated in vitro through mechanical cycling tests and has been used to predict the clinical behavior of restorations,[38] thereby simulating masticatory forces.[39] It is estimated that the mechanical cycling of 1,200,000 cycles represents 5 clinical years.[39-41] Mechanical cycling in an aqueous environment leads to stress corrosion in glass and oxide ceramics by water molecules[42] causing crack growth and decreased flexural strength of ceramic materials compared to testing in a dry environment.[43,44] Studies report that water degradation accelerates crack growth in dental ceramics, which leads to premature failure of ceramic restorations.[45,46]

In addition to the slow crack growth, 3Y-TZP can present an accelerated tetragonal to monoclinic phase transformation when submitted to different scenarios, such as high temperature,[47] contact with water,[48,49] or low temperature,[50] leading to superficial microcracks. This phenomenon is called hydrothermal aging. It was observed that zirconia underwent a degradation process when aged in the mouth for a period of 1 year and that the increase in the monoclinic phase percentage was similar to a zirconia aged in an autoclave.[49] Some studies have also varied the mechanical cycling frequency in addition to different types of aging, and it has been observed that aging causes a decrease in the flexural strength of ceramics.[42] In some cases, the ceramic's fracture resistance can increase following fewer loading cycles (20,000 cycles), depending on the ceramic composition and the processing method,[51] or can remain unchanged following cyclic loading up to 100,000 cycles.[52] Thus, 10^6 cycles were performed for the present study, as this is considered by the literature to be sufficient for the mechanical degradation results to be reliable.[53]

The first hypothesis that the porcelain-to-zirconia ratios of the stress-free bilayer CAD/CAM ceramic groups affect their flexural strength was rejected. A minimum thickness of 0.3 to

0.5 mm[27] is generally required for zirconia frameworks, depending on the region and the CAD/CAM system used. One of the advantages of the reduced thickness (0.3 mm) is the conservation of the dental structure[27] and the ceramic's improved translucency. On the other hand, the higher thickness of the covering ceramic[54] associated with rapid cooling[55] are important factors that predispose the veneering ceramic to fracture, also called chipping.[56] Ceramic veneer thicknesses > 1 mm reduce the flexural strength of bilayers.[15] The greater the proportion of veneering ceramic on the zirconia structure, the lower its resistance to fracture.[56] Some studies report that zirconia with a smaller thickness will present a better resistance to the propagation of defects near the porcelain-zirconia interface[54]; thus, the maximum stress location can change from the surface to the interface, depending on the veneer–core thickness ratio.[25] The interface between ceramics and zirconia is sensitive to heat transfer between the materials,[57] and the porcelain fractures when thick porcelain layers are used due to less thermal diffusion.[57] However, changes in the firing cycles of VM 9 ceramics and different zirconia thicknesses (0.5, 1.0, and 5.0 mm) significantly influenced their mechanical strengths.[58]

The second hypothesis, that the bonding strategies of the stress-free bilayer CAD/CAM ceramic groups result in higher flexural strength than the conventional hand-layered technique, was partially accepted. Airborne particle abrasion with silica-coated Al_2O_3 showed lower biaxial flexural strength in both porcelain-to-zirconia ratio groups; however, the VB-SBU group presented a higher flexural strength. These results are probably related to the surface treatment rather than the framework thickness, so the surface treatment factor affects the resistance to biaxial flexure.[26] In fact, the type of surface treatment of zirconia before covering it with cemented ceramics significantly improves the strength of bilayered restorations,[59] as was the result found in the group treated with Al_20_3 and SBU. Flexural strength increased when zirconia was airborne particle–abraded with Al_20_3 or aluminum coated with silica after sintering, without the need for heat treatment after airborne particle abrasion.[60] Although 50-μm particle abrasion significantly increased biaxial flexural strength compared to sintered bilayered zirconia samples, 120-μm particle abrasion decreased flexural strength and showed a higher monoclinic phase percentage.[61] In evaluating different surface treatments for adhesion to zirconia, it was observed that the hydrothermal aging for 5 years and the mechanical cycling increased the monoclinic phase and the samples blasted with 50-μm aluminum oxide presented greater flexural resistance than samples treated with silica-coated Al_20_3 of 30 μm and the untreated group.[62] However, Souza et al[34] demonstrated that different types of particles and pressures in blasting did not influence the material's flexural strength.

Additionally, the RC and SBU experimental groups received a bonding agent containing MDP, which has a strong bond to zirconium oxides. Moreover, the vinyl group can react with monomers in resin materials, further improving adhesion.[63] Therefore, it is believed that blasting with 50-μm Al_2O_3 created a favorable roughness and uneven surfaces while the surface compressive stresses (due to phase transformation and work hardening) increased the flexural strength; however, the MDP-containing primer also contributed to the increased strength. In addition, the mechanical cycling in water under the conditions of the present study was not harmful to the adhesive interfaces.

In a similar study, Costa et al[16] observed lower BFS resistance for the conventional bilayer group (± 0.7-mm ceramic/± 0.27-mm Y-TZP) compared to the group with RLM (± 0.7-mm ceramic/± 0.27-mm Y-TZP), as the cementation of the ceramic restorations excludes the heating/cooling stresses caused by the RLM technique. The adhesive cement in anatomically correct samples can play a role in the stress distribution and the rupture of adhesive bonds. Another factor that can influence bilayer ceramic restorations' flexural strength is the manufacture of the veneering ceramic. Juntavee and Serirojanakul[64] evaluated the flexural strength of different overlay ceramic production techniques, in which the best result found was the ceramic milled in CAD/CAM. The other groups were pressed ceramics through the lost wax, where greater porosity was observed in its surface, which negatively impacts flexural strength, acting as a stress concentration point. In another study evaluating the BFS of two types of zirconia bilayer crowns (heat-pressed and sintered veneering ceramic), no statistical difference was found between the groups. However, heat pressing had fewer flaws and porosity than hand veneering, as it is a more controlled procedure compared to the sintered process, which is more sensitive and subject to variability.[65]

The absence of a control group without mechanical cycling and the application and cementation of other ceramic materials are limitations of this study. However, delamination did not occur in the cemented layers, which can be explained by the strong bond between porcelain and resin cement and the sufficient amount of bonding material between them and zirconia. Therefore, the porcelain-zirconia interfaces–whether cemented or not–still deserve investigation, including other adhesive and cementation techniques, as well as clinical research that evaluates long-term behavior, as it is fundamental to establish the ideal surface treatment for these materials.

CONCLUSIONS

Based on the results, it can be concluded that the zirconia bonding strategy with airborne-particle abrasion using 50-μm Al_2O_3 followed by a primer application increases the flexural strength of the bilayer CAD/CAM ceramic system regardless of the porcelain-to-zirconia thickness ratio. Thus, a stress-free bilayer CAD/CAM ceramic system with a feldspathic ceramic veneer bonded to a zirconia framework seems to be a viable alternative to conventional hand-veneered zirconia restorations.

ACKNOWLEDGMENTS

The authors are thankful to Dr Ivan Balduci for the statistical analysis. This study was supported by the Fundação de Amparo à Pesquisa do Estado de São Paulo – FAPESP, Brazil, (n0 2012/02945-0). Y.Z. would like to thank the United States National Institutes of Health / National Institute of Dental and Craniofacial Research for their support (grants No. R01 DE026772 and R01 DE026279). The authors report no conflicts of interest.

REFERENCES

1. Guazzato M, Albakry M, Ringer SP, Swain MV. Strength, fracture toughness and microstructure of a selection of all-ceramic materials. Part II. Zirconia-based dental ceramics. Dent Mater 2004;20:449–456. [PubMed: 15081551]
2. Bachhav VC, Aras MA. Zirconia-based fixed partial dentures: A clinical review. Quintessence Int 2011;42:173–182. [PubMed: 21359252]

3. Zhang Y, Kelly JR. Dental ceramics for restoration and metal-veneering. Dent Clin North Am 2017;61:797–819. [PubMed: 28886769]
4. Zhang Y, Lawn BR. Novel zirconia materials in dentistry. J Dent Res 2018;97:140–147. [PubMed: 29035694]
5. Hüttig F, Keitel JP, Prutscher A, Spintzyk S, Klink A. Fixed dental prostheses and single-tooth crowns based on ceria-stabilized tetragonal zirconia/alumina nanocomposite frameworks: Outcome after 2 years in a clinical trial. Int J Prosthodont 2017;30:461–464. [PubMed: 28806427]
6. Miura S, Kasahara S, Yamauchi S, et al. Clinical evaluation of zirconia-based all-ceramic single crowns: An up to 12-year retrospective cohort study. Clin Oral Investig 2018;22:697–706.
7. Sailer I, Fehér A, Filser F, et al. Prospective clinical study of zirconia posterior fixed partial dentures: 3-year follow-up. Quintessence Int 2006;37:685–693. [PubMed: 17017630]
8. Sailer I, Fehér A, Filser F, Gauckler LJ, Lüthy H, Hämmerle CH. Five-year clinical results of zirconia frameworks for posterior fixed partial dentures. Int J Prosthodont 2007;20:383–388. [PubMed: 17695869]
9. Hung CY, Huang YS. Effect of veneering techniques on ceramic fracture of zirconia restoration. J Prosthodont Implantol 2012;1:66–70.
10. Pang Z, Chughtai A, Sailer I, Zhang Y. A fractographic study of clinically retrieved zirconia-ceramic and metal-ceramic fixed dental prostheses. Dent Mater 2015;31:1198–1206. [PubMed: 26233469]
11. Swain MV. Unstable cracking (chipping) of veneering porcelain on all-ceramic dental crowns and fixed partial dentures. Acta Biomater 2009;5:1668–1677. [PubMed: 19201268]
12. Kim J, Dhitala S, Zhivagob P, Kaizer MR, Zhang Y. Viscoelastic finite element analysis of residual stresses in porcelain-veneered zirconia dental crowns. J Mech Behav Biomed Mater 2018;82:202–209. [PubMed: 29621687]
13. Dhital S, Rodrigues C, Zhang Y, Kim J. Viscoelastic finite element evaluation of transient and residual stresses in dental crowns: Design parametric study. J Mech Behav Biomed Mater 2020;103:103545. [PubMed: 31760273]
14. Guess PC, Kulis A, Witkowski S, Wolkewitz M, Zhang Y, Strub JR. Shear bond strengths between different zirconia cores and veneering ceramics and their susceptibility to thermocycling. Dent Mater 2008;24:1556–1567. [PubMed: 18466964]
15. Lima JM, Souza AC, Anami LC, Bottino MA, Melo RM, Souza RO. Effects of thickness, processing technique, and cooling rate protocol on the flexural strength of a bilayer ceramic system. Dent Mater 2013;29:1063–1072. [PubMed: 23957933]
16. Costa AK, Borges AL, Fleming GJ, Addison O. The strength of sintered and adhesively bonded zirconia/veneer-ceramic bilayers. J Dent 2014;42:1269–1276. [PubMed: 25132365]
17. Kim JW, Kim JH, Thompson VP, Zhang Y. Sliding contact fatigue damage in layered ceramic structures. J Dent Res 2007;86:1046–1050. [PubMed: 17959894]
18. Harada K, Raigrodski AJ, Chung KH, Flinn BD, Dogan S, Mancl LA. A comparative evaluation of the translucency of zirconias and lithium disilicate for monolithic restorations. J Prosthet Dent 2016;116:257–263. [PubMed: 26994676]
19. Zhang Y. Making yttria-stabilized tetragonal zirconia translucent. Dent Mater 2014;30:1195–1203. [PubMed: 25193781]
20. Alessandretti R, Ribeiro R, Borba M, Bona AD. Fracture load and failure mode of CAD-on ceramic structures. Braz Dent J 2019;30:380–384. [PubMed: 31340229]
21. Lee JJ, Wang Y, Lloyd IK, Lawn BR. Joining veneers to ceramic cores and dentition with adhesive interlayers. J Dent Res 2007;86:745–748. [PubMed: 17652203]
22. Kobayashi K, Komine F, Blatz MB, Saito A, Koizumi H, Matsumura H. Influence of priming agents on the short-term bond strength of an indirect composite veneering material to zirconium dioxide ceramic. Quintessence Int 2009;40:545–555. [PubMed: 19626228]
23. International Organization for Standardization. ISO 6872:2015. Dentistry–Ceramic materials. Geneva: ISO, 2015.
24. Hsueh CH, Thompson GA, Jadaan OM, Wereszczak AA, Becher PF. Analyses of layer-thickness effects in bilayered dental ceramics subjected to thermal stresses and ring-on-ring tests. Dent Mater 2008;24:9–17. [PubMed: 17379295]

25. Hsueh CH, Luttrell CR, Becher PF. Analyses of multilayered dental ceramics subjected to biaxial flexure tests. Dent Mater 2006;22:460–469. [PubMed: 16099028]
26. Borba M, de Araujo MD, de Lima E, et al. Flexural strength and failure modes of layered ceramic structures. Dent Mater 2011;27:1259–1266. [PubMed: 21982199]
27. Yi YJ, Kelly JR. Effect of occlusal contact size on interfacial stresses and failure of a bonded ceramic: FEA and monotonic loading analyses. Dent Mater 2008;24:403–409. [PubMed: 17698187]
28. Fabris D, Souza JC, Silva FS, et al. The bending stress distribution in bilayered and graded zirconia-based dental ceramics. Ceram Int 2016;42:11025–11031. [PubMed: 28104926]
29. Nam MG, Park MG. Changes in the flexural strength of translucent zirconia due to glazing and low-temperature degradation. J Prosthet Dent 2018;120:969.e1–969.e6.
30. Kurtulmus-Yilmaz S, Aktore H. Effect of the application of surface treatments before and after sintering on the flexural strength, phase transformation and surface topography of zirconia. J Dent 2018;72:29–38. [PubMed: 29501794]
31. Silva FP, Vilela ALR, Almeida MMG, Oliveira ARF, Raposo LHA, Menezes MS. Surface topography, gloss and flexural strength of pressable ceramic after finishing-polishing protocols. Braz Dent J 2019;30:164–170. [PubMed: 30970060]
32. Uwalaka CO, Karpukhina N, Cao X, Bissasu S, Wilson RM, Cattell MJ. Effect of sandblasting, etching and resin bonding on the flexural strength/bonding of novel glass-ceramics. Dent Mater 2018;34:1566–1577. [PubMed: 30072165]
33. Thompson GA. Determining the slow crack growth parameter and Weibull two-parameter estimates of bilaminate discs by constant displacement-rate flexural testing. Dent Mater 2004;20:51–62. [PubMed: 14698774]
34. Souza RO, Valandro LF, Melo RM, Machado JP, Bottino MA, Ozcan M. Air-particle abrasion on zirconia ceramic using different protocols: Effects on biaxial flexural strength after cyclic loading, phase transformation and surface topography. J Mech Behav Biomed Mater 2013;26:155–159. [PubMed: 23746698]
35. Murillo-Gómez F, Wanderley RB, De Goes MF. Impact of silane-containing universal adhesive on the biaxial flexural strength of a resin cement/glass-ceramic system. Operative Dent 2019;44:200–209.
36. Pereira GKR, Guilardi LF, Dapieve KS, Kleverlaan CJ, Rippe MP, Valandro LF. Mechanical reliability, fatigue strength and survival analysis of new polycrystalline translucent zirconia ceramics for monolithic restorations. J Mech Behav Biomed Mater 2018;85:57–65. [PubMed: 29857261]
37. Wiskott HW, Nicholls JI, Belser UC. Stress fatigue: Basic principles and prosthodontic implications. Int J Prosthodont 1995;8:105–116. [PubMed: 7575960]
38. Mallmann F, Rosa L, Borba M, Della Bona A. Effect of screw-access hole and mechanical cycling on fracture load of 3-unit implant-supported fixed dental prostheses. J Prosthet Dent 2018;119:124–131. [PubMed: 28477919]
39. DeLong R, Douglas WH. Development of an artificial oral environment for the testing of dental restoratives: Bi-axial force and movement control. J Dent Res 1983;62:32–36. [PubMed: 6571851]
40. Att W, Grigoriadou M, Strub JR. ZrO2 three-unit fixed partial dentures: Comparison of failure load before and after exposure to a mastication simulator. J Oral Rehabil 2007;34:282–290. [PubMed: 17371566]
41. Zhang Y, Lawn BR, Rekow ED, Thompson VP. Effect of sandblasting on the long-term performance of dental ceramics. J Biomed Mater Res B Appl Biomater 2004;71:381–386. [PubMed: 15386395]
42. Cotes C, Arata A, Melo RM, Bottino MA, Machado JP, Souza RO. Effects of aging procedures on the topographic surface, structural stability, and mechanical strength of a ZrO2-based dental ceramic. Dent Mater 2014;30:e396–e404. [PubMed: 25244926]
43. Kelly JR. Perspectives on strength. Dent Mater 1995;11:103–110. [PubMed: 8621029]
44. De Aza AH, Chevalier J, Fantozzi G, Schehl M, Torrecillas R. Crack growth resistance of alumina, zirconia and zirconia toughened alumina ceramics for joint prostheses. Biomaterials 2002;23:937–945. [PubMed: 11774853]

45. Chevalier J. What future for zirconia as a biomaterial?. Biomaterials. 2006;27:535–543. [PubMed: 16143387]
46. Zhang Y, Sailer I, Lawn BR. Fatigue of dental ceramics. J Dent 2013;41:1135–1147. [PubMed: 24135295]
47. Sato T, Shimada M. Transformation of yttria-doped tetragonal ZrO2 polycrystals by annealing in water. J Am Ceram Soc 1985;68:3.
48. Studart AR, Filser F, Kocher P, Gauckler LJ. Fatigue of zirconia under cyclic loading in water and its implications for the design of dental bridges. Dent Mater 2007;23:106–114. [PubMed: 16473402]
49. Vila-Nova TEL, Gurgel de Carvalho IH, Moura DMD, et al. Effect of finishing/polishing techniques and low temperature degradaation on the surface topography, phase transformation and flexural strength of ZrO2 ceramic. Dent Mater 2020;36:e126–e139. [PubMed: 32008750]
50. Amaral M, Cesar PF, Bottino MA, Lohbauer U, Valandro LF. Fatigue behavior of Y-TZP ceramic after surface treatments. J Mech Behav Biomed Mater 2016;57:149–156. [PubMed: 26717249]
51. Nemli SK, Yilmaz H, Aydin C, Bal BT, Tıraş T. Effect of fatigue on fracture toughness and phase transformation of Y-TZP ceramics by X-ray diffraction and Raman spectroscopy. J Biomed Mater Res B Appl Biomater 2011;100:416–424. [PubMed: 22102326]
52. Souza RO, Valandro LF, Melo RM, Machado JP, Bottino MA, Ozcan M. Air-particle abrasion on zirconia ceramic using different protocols: Effects on biaxial flexural strength after cyclic loading, phase transformation and surface topography. J Mech Behav Biomed Mater 2013;26:155–163. [PubMed: 23746698]
53. Wiskott HW, Nicholls JI, Belser UC. Stress fatigue: Basic principles and prosthodontic implications. Int J Prosthodont 1995;8:105–116. [PubMed: 7575960]
54. Figueiredo VMG, Pereira SMB, Bressiani E, et al. Effects of porcelain thickness on the flexural strength and crack propagation in a bilayered zirconia system. J Appl Oral Sci 2017;25:566–574. [PubMed: 29069155]
55. Tang YL, Kim JH, Shim JS, Kim S. The effect of different cooling rates and coping thicknesses on the failure load of zirconia-ceramic crowns after fatigue loading. J Adv Prosthodont 2017;9:152–158. [PubMed: 28680545]
56. Kim JH, Ko KH, Huh YH, Park CJ, Cho LR. Effects of the thickness ratio of zirconia-lithium disilicate bilayered ceramics on the translucency and flexural strength. J Prosthodont 2020;29:334–340. [PubMed: 31876065]
57. Zhang Y, Allahkarami M, Hanan JC. Measuring residual stress in ceramic zirconia-porcelain dental crowns by nanoindentation. J Mech Behav Biomed Mater 2012;6:120–127. [PubMed: 22301181]
58. Alayad AS. Effect of zirconia core thickness and veneer firing cycle on the biaxial flexural strength of veneering ceramic. J Prosthodont 2020;29:26–33. [PubMed: 29968266]
59. Aboushelib MN, Wang H. Influence of crystal structure on debonding failure of zirconia veneered restorations. Dent Mater 2013;29:e97–e102. [PubMed: 23694843]
60. Prasad HA, Pasha N, Hilal M, et al. To evaluate effect of airborne particle abrasion using different abrasives particles and compare two commercial available zirconia on flexural strength on heat treatment. Int J Biomed Sci 2017;13:93–112. [PubMed: 28824346]
61. Garcia Fonseca R, de Oliveira Abi-Rached F, dos Santos Nunes Reis JM, Rambaldi E, Baldissara P. Effect of particle size on the flexural strength and phase transformation of an airborne-particle abraded yttria-stabilized tetragonal zirconia polycrystal ceramic. J Prosthet Dent 2013;110:510–514. [PubMed: 24182897]
62. Kelch M, Schulz J, Edelhoff D, Sener B, Stawarczyk B. Impact of different pretreatments and aging procedures on the flexural strength and phase structure of zirconia ceramics. Dent Mater 2019;35:1439–1449. [PubMed: 31399228]
63. Mehta D, Shetty R. Bonding to zirconia: Elucidating the confusion. Int Dent SA 2010;12:46–52.
64. Juntavee N, Serirojanakul P. Influence of different veneering techniques and thermal tempering on flexural strength of ceramic veneered yttria partially stabilized tetragonal zirconia polycrystalline restoration. J Clin Exp Dent 2019;11:e421–e431. [PubMed: 31275514]

65. Tsalouchou E, Cattell MJ, Knowles JC, Pittayachawan P, McDonald A. Fatigue and fracture properties of yttria partially stabilized zirconia crown systems. Dent Mater 2008;24:308–318. [PubMed: 17681371]

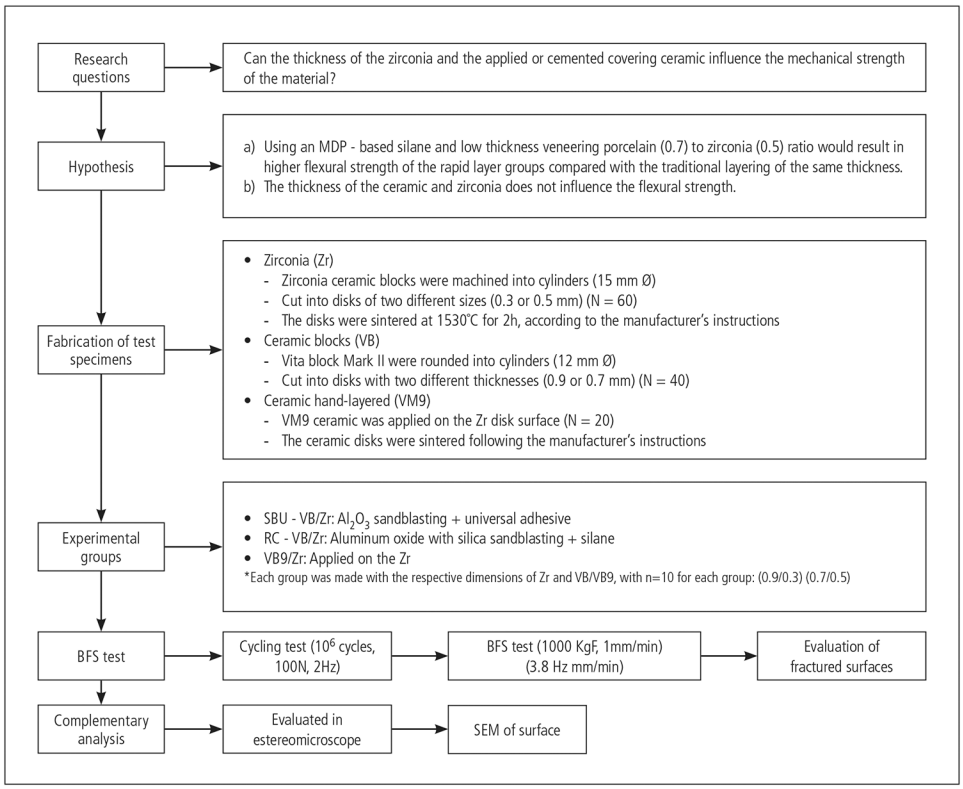

Fig 1.
Flowchart of the study design.

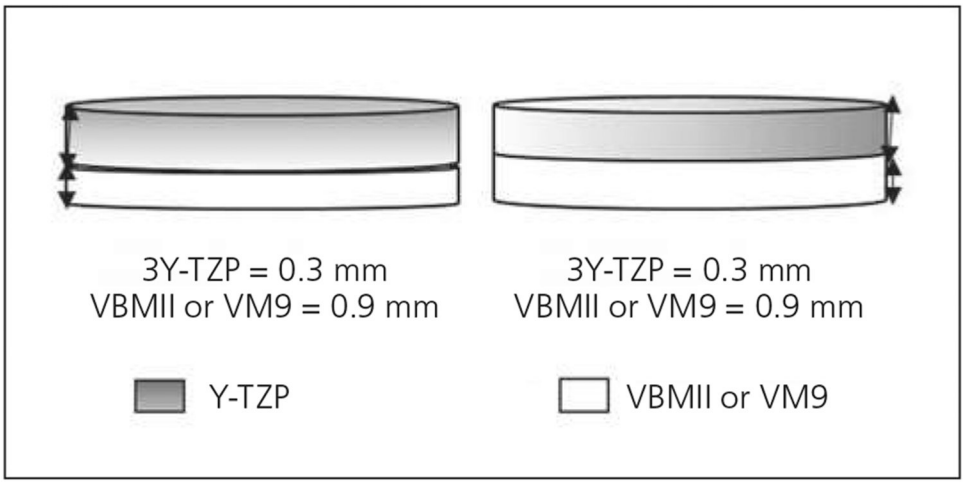

Fig 2.

Experimental groups: 3Y-TZP of 0.3- or 0.5-mm thickness, feldspar ceramic block of 0.9- or 0.7-mm thickness, and ceramic veneer applied on the 3Y-TZP discs.

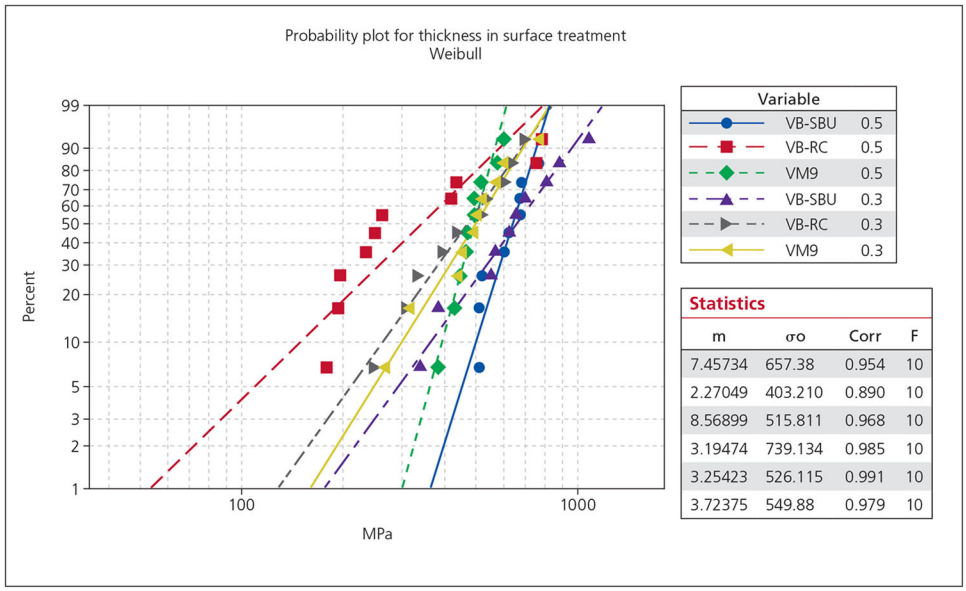

Fig 3.
Weibull plot for biaxial flexural strength data of all groups.

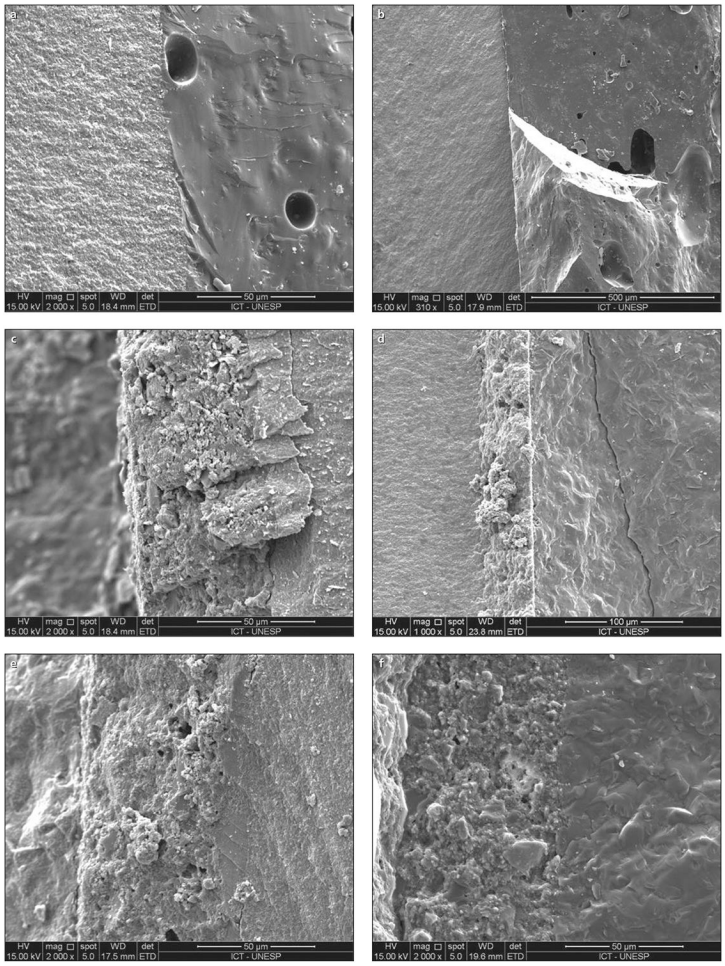

Fig 4.

SEM analysis of the interfaces from each group (x2,000 magnification). *(a)* VM 9/Zr (0.9: 0.3). *(b)* VM 9/Zr (0.7: 0.5). *(c)* VB/Zr-SBU (0.9: 0.3). *(d)* VB/Zr-SBU (0.7: 0.5). *(e)* VB/Zr-RC (0.9: 0.3). *(f)* VB/Zr-RC (0.7: 0.5).

Table 1

Materials Used in the Study

Material	Commercial name	Manufacturer	Composition*	Batch #
3Y-TZP zirconium oxide blocks	VITA In-Ceram YZ Cubes	VITA Zahnfabrik	ZrO_2; Y_2O_3; HfO_2; Al_2O_3; SiO_2; Na_2O	38320
Feldspar ceramic	VM 9	VITA Zahnfabrik	SiO_2, Al_2O_3, K_2O, Na_2O, TiO_2, CeO_2, ZrO_2, CaO, B_2O_3, BaO, SnO_2, Mg, Fe, and P oxides	12470
Feldspar ceramic block	Vitablocs Mark II	VITA Zahnfabrik	SiO_2; Al_2O_3; Na_2O; K_2O; CaO; TiO_2	21401
Silane	Monobond Plus	Ivoclar Vivadent	Alcohol solution of silane methacrylate, phosphoric acid methacrylate, and sulphide methacrylate	R50513
Universal adhesive	ScotchBond Universal	3M ESPE	MDP phosphate monomer, dimethacrylate resins, HEMA, Vitrebond copolymer, filler, ethanol, water, initiators, silane	507329
Condac Porcelana	Hydrofluoric acid 5%	FGM	HF 5% (water, thickener, surfactant, dye)	N/A
Silica-coated aluminum oxide	Rocatec Soft	3M ESPE	High-purity aluminum oxide 30 μm, modified with silica (SiO_2)	13040104781506373
Aluminum oxide powder	Aluminum oxide	Bio Art	Al_2O_3 (50 μm)	N/A
Resin cement	Panavia F 2.0	Kuraray Noritake	Paste A: MDP, hydrophobic and hydrophilic dimethacrylate, benzoyl peroxide, camphoroquinone, coloidalsilica	051234
			Paste B: sodium fluoride, hydrophobic and hydrophilic dimethacrylate, diethanol-p-toluidine, T-isopropylicbenzenic sodium sulfinate, barium glass, titanium dioxide, coloidal silica	

ZrO_2 = zirconium dioxide; Y_2O_2 = yttrium dioxide; HfO_2 = hafnium oxide; Al_2O_3 = aluminum oxide; SiO_2 = silicon dioxide; Na_2O = sodium oxide; K_2O = potassium oxide; Na_2O = sodium oxide; TiO_2 = titanium dioxide; CeO_2 = cerium oxide; CaO = calcium oxide; B_2O_3 = boron oxide; BaO = barium oxide; SnO_2 = tin oxide; Mg = magnesium; Fe = iron; P = phosphorus.

*According to the information from the manufacturers' official websites.

Table 2

Sintering Cycle for VM 9 Ceramic According to the Manufacturer's Instructions

Initial temperature (°C)	Drying time (min)	Heating rate (°C/min)	Initial temperature under vacuum (°C)	Final temperature under vacuum (°C)	Vacuum time (min)
500	2	60	500	950	8

Table 3

Results of Two-Way ANOVA for Biaxial Flexural Strength Data

Source	df	SS	MS	F	*P*
Bonding strategy	2	700,337	350,168	20.66	.0000 *
Porcelain: zirconia ratio	1	64,886	64,886	3.83	.0556
Bonding strategy and porcelain: zirconia ratio	2	35,962	17,981	1.06	.3533
Error	54	915,473	16,953		
Total	59	1,716,657			

df = degrees of freedom; SS = sum of squares; MS = mean square.

* Significant ($P < .05$).

Table 4

Flexural Strength (MPa), Weibull modulus (m), Characteristic Strength (σo), and 95% CI Biaxial Flexural Strength of Experimental Groups

Porcelain: zirconia ratio	Bonding strategy	Group name	Flexural strength (MPa)	Weibull modulus (m)	95% CI	Weibull characteristic strength	95% CI
0.7: 0.5 mm	Aluminum oxide + SBU	VB/Zr-SBU	636.55 ± 98.02 $^{\alpha}$	7.45 ^{A}	4.412.6	675.3 ^{a}	618.6–737.2
	Silica-coated aluminum oxide	VB/Zr-RC	344.05 ± 98.02 $^{\beta}$	4.8 ^{A}	2.38.7	373.5 ^{c}	326.8–426.9
	No surface treatment	VM/Zr (control)	489.25 ± 66.45 $^{\gamma}$	8.5 ^{A}	5.613.0	515.8 ^{b}	477.5–557.1
0.9: 0.3 mm	Aluminum oxide + SBU	VB/Zr-SBU	698.4 ± 194.85 $^{\alpha}$	4.8 ^{A}	2.56.3	767.5 ^{a}	652.1–903.3
	Silica-coated aluminum oxide	VB/Zr-RC	471.48 ± 151.82 $^{\beta}$	3.2 ^{A}	1.75.9	526.1 $^{a\,b\,c}$	430.4–642.9
	No surface treatment	VM/Zr (control)	497.33 ± 143.15 $^{\beta}$	3.7 ^{A}	2.26.2	549.8 $^{a\,b}$	461.3–655.4

Different uppercase superscript letters indicate significant differences in Weibull moduli among the groups, and different lowercase superscript letters indicate significant differences in characteristic strength among groups. Different superscript symbols indicate differences in flexural strength.